INORGANIC CHEMISTRY
FRONTIERS

RESEARCH ARTICLE

View Article Online
View Journal

Cite this: DOI: 10.1039/d5qi02482j

Bridging the gap: thymine segments to create single-stranded versions of DNA_2-$[Ag_{16}Cl_2]^{8+}$

Vanessa Rück, *†[a] Hiroki Kanazawa, †[b] Zhiyu Huang, [a] Christian Brinch Mollerup, [c] Leila Lo Leggio, [a] Jiro Kondo *[b] and Tom Vosch *[a]

Significant effort has been invested into unraveling the structure–property relationship of DNA-AgNCs using relatively short DNA sequences. Due to the limited sequence length, two or more strands are often required to stabilize a DNA-AgNC. Therefore, functionalization inherently introduces multiple reactive sites, hindering the implementation of single-site linking strategies. Here, we exploit the concept of using a thymine linking segment to connect two small DNA strands to develop a single-stranded version of DNA_2-$[Ag_{16}Cl_2]^{8+}$. Our results demonstrate that these redesigned constructs preserve the core AgNC structure and photophysical properties while enabling future single-site functionalization. Furthermore, this approach allows for experimental verification that the DNA linking segments do not interfere with AgNC formation.

Received 9th December 2025,
Accepted 8th January 2026

DOI: 10.1039/d5qi02482j

rsc.li/frontiers-inorganic

Introduction

DNA-stabilized silver nanoclusters (DNA-AgNCs) are a unique class of fluorescent emitters that were first reported by Petty *et al.* in 2004.[1] These nanoclusters consist of a limited number of silver atoms and cations (typically 2–30), coordinated and stabilized with one or more single-stranded DNA oligomers.[2] DNA-AgNCs exhibit tunable emission spanning the visible to near-infrared (NIR) spectral range and are often characterized by high fluorescence quantum yields, large Stokes shifts, and good chemical and photostability.[3–6] Due to their favourable optical properties, DNA-AgNCs are promising candidates for fluorescence imaging applications.[7–9] Despite this potential, limited work has been done on developing and testing conjugation strategies of DNA-AgNCs for labelling applications.[8,10,11] Such functionalization is essential for enabling specific target labelling and thereby unlocking the full potential of DNA-AgNCs as fluorophores. A key challenge lies in the possibility that introducing functional groups may interfere with the DNA–silver core interactions, potentially altering the photophysical properties or compromising the structural stability of the nanoclusters.

The current library of DNA sequences used for colour-specific stabilization of AgNCs consists mainly of strands that are about ten nucleobases long.[12,13] As a result, most AgNCs are stabilized with two DNA strands.[12,14–16] Although single, longer DNA strands can also stabilize AgNCs,[17] using two shorter strands offers advantages, such as a more confined screening space for machine learning algorithms[18] and the ability to introduce structural symmetry. A prominent example is the well-studied DNA_2-$[Ag_{16}Cl_2]^{8+}$ nanocluster, which has become one of the best understood DNA-AgNC systems to date.[19–21]

Rück *et al.* demonstrated the site-specific conjugation of the purified DNA_2-$[Ag_{16}Cl_2]^{8+}$ nanocluster to three different peptides and a small protein using strain-promoted azide–alkyne cycloaddition (SPAAC), a copper-free click reaction eliminating the need for a copper catalyst.[8] This approach enabled efficient and stable linkage of biomolecules to DNA_2-$[Ag_{16}Cl_2]^{8+}$ without compromising their photophysical properties. In bioimaging experiments using Chinese hamster ovary (CHO) cells, specific labeling of human insulin receptors at the cell membrane was achieved.[8] Notably, the nanoclusters maintained their spectral characteristics, highlighting their suitability for bioimaging applications. However, using two DNA strands inherently introduces two conjugation sites, which can cause potential cross-linking of binding sites and hence a non-linear fluorescence response. Thus, a single-site labeling strategy with one functional group to one binding site is more desirable.

Stabilizing $[Ag_{16}Cl_2]^{8+}$ with a single DNA strand is challenging, and to the best of our knowledge, this has not yet been

[a]Department of Chemistry, University of Copenhagen, Universitetsparken 5, DK-2100 Copenhagen, Denmark. E-mail: vr@chem.ku.dk, tom@chem.ku.dk
[b]Department of Materials and Life Sciences, Sophia University, 7-1 Kioi-cho, Chiyoda-ku, 102-8554 Tokyo, Japan. E-mail: j.kondo@sophia.ac.jp
[c]Department of Forensic Medicine, University of Copenhagen, Frederik V's Vej 11, DK-2100 Copenhagen, Denmark
†These authors contributed equally.

achieved for red- or NIR-emitting AgNCs. We note, however, that a few examples of smaller green emissive AgNCs have been reported in the literature.[22,23]

In this work, we address this challenge by designing a single-stranded version of the DNA_2-$[Ag_{16}Cl_2]^{8+}$ system, created by connecting the two original DNA sequences with thymine linkers of four, five and six nucleobases. These linker lengths were rationally chosen based on the available crystal structure.[19] As a result, we obtained a single oligonucleotide that preserves the nanocluster's structural integrity and photophysical properties. Such single-stranded architecture enables controlled, single-site functionalization, enhances labeling specificity, and supports the development of targeted fluorescent probes for bioimaging.[8]

Two crystal structures show that the Ag_{16} cluster core remains structurally consistent in these redesigned single-stranded variants. Together with mass spectroscopy analyses, these findings experimentally confirm that the small thymine bridge is suitable as a linking segment. This approach could also be used to screen other four- to six nucleotide segments to check if they do not interfere with AgNC formation.

Results and discussion

The original DNA_2-$[Ag_{16}Cl_2]^{8+}$ structure is stabilized using two 5′-CACCTAGCGA-3′ oligomers.[19] Based on the crystal structure, we can see that the 3′-end of oligomer 1 and the 5′-end of oligomer 2 are relatively close. In order to connect these two ends, we used three different spacer lengths consisting of four, five and six thymines, which have been suggested in the literature to have the least affinity to the silver cations of the natural nucleobases.[24] These single-stranded sequences will be further referred to as 2xDNA(T_4), 2xDNA(T_5), and 2xDNA(T_6).

Synthesis of DNA-AgNCs using 24–26 nucleotide single-stranded sequences was performed as previously reported.[19] Briefly, the oligomer strands were mixed with $AgNO_3$ in 10 mM ammonium acetate (NH_4OAc), and a freshly prepared $NaBH_4$ solution was added after an incubation time of 15 min to promote cluster formation. The final ratio between the components was $[DNA]:[AgNO_3]:[NaBH_4]$ = 25 μM : 187.5 μM : 93.75 μM. After 7 days at 4 °C, the absorption spectra of the unpurified sample were recorded to verify the formation of the cluster. Fig. S1A shows that all three samples form the desired $[Ag_{16}Cl_2]^{8+}$ cluster; however, the best yield is achieved with the T_6 spacer length.

Based on previous observations, the addition of sodium chloride (NaCl) can improve the yield of $[Ag_{16}Cl_2]^{8+}$ cluster formation.[21,25] Therefore, NaCl tests were carried out for the clusters with T_6 spacers. Different concentrations of NaCl (10, 30 and 50 mM) were added during the synthesis procedure. The best results were obtained with a NaCl concentration of 30 mM, see Fig. S1B. The addition of 50 mM NaCl did not result in a significantly higher yield than with 30 mM. Hence, a mixture of 10 mM NH_4OAc with 30 mM NaCl was used for the synthesis. After a 7-day reaction period, the mixture was purified by high-performance liquid chromatography (HPLC), yielding successful separation for all three cases. Details on the HPLC purification and the corresponding chromatograms can be found in the SI (Fig. S2–S4).

The spectroscopic characterization of the purified 2xDNA(T_4)-$[Ag_{16}Cl_2]^{8+}$, 2xDNA(T_5)-$[Ag_{16}Cl_2]^{8+}$ and 2xDNA(T_6)-$[Ag_{16}Cl_2]^{8+}$ nanoclusters shows that the photophysical properties remain nearly unaltered by the different spacer lengths, see Fig. 1 and Table 1. The absorption maximum remains at around 524 nm. However, compared to the original DNA_2-$[Ag_{16}Cl_2]^{8+}$ nanocluster, the emission maxima are slightly red-shifted, now centred at around 750 nm. The average fluorescence decay time and fluorescence quantum yield are also very similar and seem not to be affected by the spacers (see Table 1). Time-resolved fluorescence anisotropy measurements were used to determine the hydrodynamic volume. Compared to DNA_2-$[Ag_{16}Cl_2]^{8+}$, the hydrodynamic volume increases with increasing spacer length. While some increase is expected, the significant increase might indicate substantial drag of the thymine segment in solution.

Additionally, the single-stranded silver nanocluster versions were analysed by electrospray ionization mass spectrometry (ESI-MS) to verify whether the AgNCs are compositionally con-

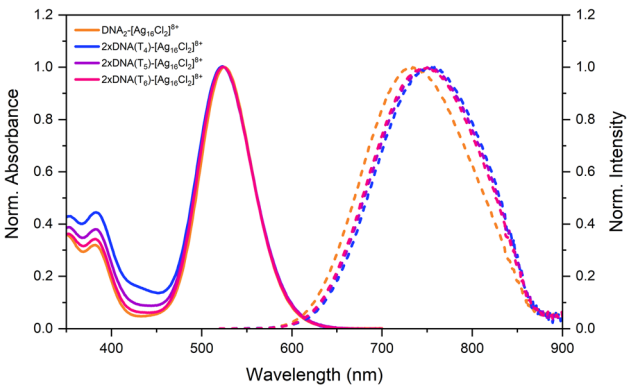

Fig. 1 Normalized absorption and emission spectra of DNA_2-$[Ag_{16}Cl_2]^{8+}$, 2xDNA(T_4)-$[Ag_{16}Cl_2]^{8+}$, 2xDNA(T_5)-$[Ag_{16}Cl_2]^{8+}$ and 2xDNA(T_6)-$[Ag_{16}Cl_2]^{8+}$ in 10 mM NH_4OAc at room temperature.

Table 1 Photophysical properties of the original DNA_2-$[Ag_{16}Cl_2]^{8+}$ and single-stranded 2xDNA(T_4)-$[Ag_{16}Cl_2]^{8+}$, 2xDNA(T_5)-$[Ag_{16}Cl_2]^{8+}$ and 2xDNA(T_6)-$[Ag_{16}Cl_2]^{8+}$ versions.

	Abs (nm)	Em (nm)	$\langle\tau\rangle$ (ns)	QY	ϕ_r (ns)	V_h (nm^3)
DNA_2	525	736	3.26	0.26	2.19	10.14
2xDNA(T_4)	524	753	3.31	0.21[a]	3.09	14.31
2xDNA(T_5)	524	750	3.46	0.23[a]	3.45	15.97
2xDNA(T_6)	523	747	3.44	0.24[a]	3.67	16.99

DNA_2 sequence: 5′-CACCTAGCGA-3′. 2xDNA(T_4) sequence: 5′-CACCTAGCGATTTTCACCTAGCGA-3′. 2xDNA(T_5) sequence: 5′-CACCTAGCGATTTTTCACCTAGCGA-3′. 2xDNA(T_6) sequence: 5′-CACCTAGCGATTTTTTCACCTAGCGA-3′. [a] Values were determined from a single point measurement (see the SI for details). For 2xDNA(T_6)-$[Ag_{16}Cl_2]^{8+}$ a multi-point measurement as also available in the SI.

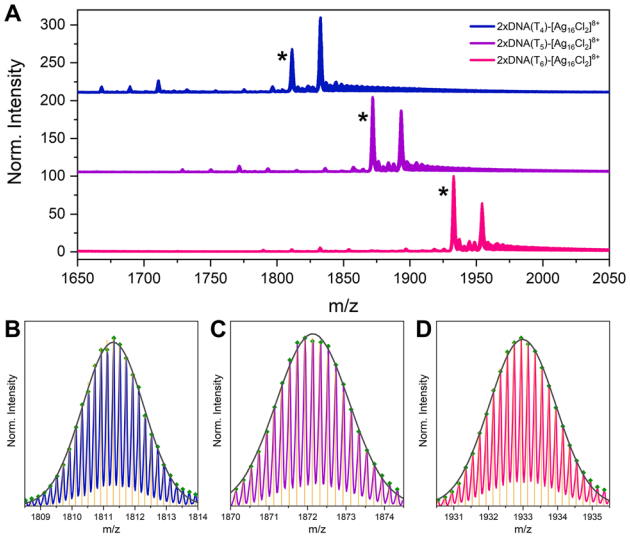

Fig. 2 (A) Mass spectra (zoom-in view) of the $z = 5^-$ regions of 2xDNA(T_4)-$[Ag_{16}Cl_2]^{8+}$, 2xDNA(T_5)-$[Ag_{16}Cl_2]^{8+}$ and 2xDNA(T_6)-$[Ag_{16}Cl_2]^{8+}$ in 10 mM NH_4OAc at room temperature displayed with offsets. (B–D) Theoretical isotopic distribution fit (yellow) along with experimental data of 2xDNA(T_4)-$[Ag_{16}Cl_2]^{8+}$ (blue), 2xDNA(T_5)-$[Ag_{16}Cl_2]^{8+}$ (purple) and 2xDNA(T_6)-$[Ag_{16}Cl_2]^{8+}$ (pink) for the highlighted peaks in (A). The dark gray line represents the Gaussian fit, while the green dots indicate the peaks used for the fit. The corresponding mean values are μ = 1811.3, 1872.1, and 1933.0 for (B), (C), and (D), respectively.

sistent with the original DNA_2-$[Ag_{16}Cl_2]^{8+}$ nanocluster. The mass spectra of all three modifications are reported in Fig. 2 and S5. The experimental mass data, highlighted in Fig. 2A, are aligned with the theoretical isotopic distribution of a compound comprising one DNA strand, 2 chloride atoms, and 16 silver atoms with an overall charge of +8. These findings are in line with the spectroscopic characterization that all three modifications form similar emitters. The second dominant molecular ion peaks correspond to a similar compound with one additional silver cation (see also Fig. S6). The presence of additional silver cations has been observed previously, and they are presumed not to be part of the AgNC core.[8,19] These cations most likely coordinate with the 3′-terminal adenine, as observed in the crystal structure of the original DNA_2-$[Ag_{16}Cl_2]^{8+}$ nanocluster.[19] Interestingly, the mass spectroscopy data also suggest that no silver cations are appreciably bound to the thymine linker, or at least not strongly enough to be seen in the mass spectra.

The spectroscopic and mass spectrometry data indicated that the new single-stranded 2xDNA(T_4)-$[Ag_{16}Cl_2]^{8+}$, 2xDNA(T_5)-$[Ag_{16}Cl_2]^{8+}$ and 2xDNA(T_6)-$[Ag_{16}Cl_2]^{8+}$ nanoclusters are similar to the original DNA_2-$[Ag_{16}Cl_2]^{8+}$ nanocluster. In order to facilitate a structural comparison and gain insight into the thymine region, we crystallized all three single-stranded variants. The 2xDNA(T_4)-$[Ag_{16}Cl_2]^{8+}$, 2xDNA(T_5)-$[Ag_{16}Cl_2]^{8+}$ and 2xDNA(T_6)-$[Ag_{16}Cl_2]^{8+}$ clusters all yielded pinkish crystals (see Fig. 3A–C and Fig. S10) using the hanging drop vapour method (see also the SI). All crystals displayed an emission maximum at around 740 nm (Fig. S11) and nanosecond-lived fluorescence decay

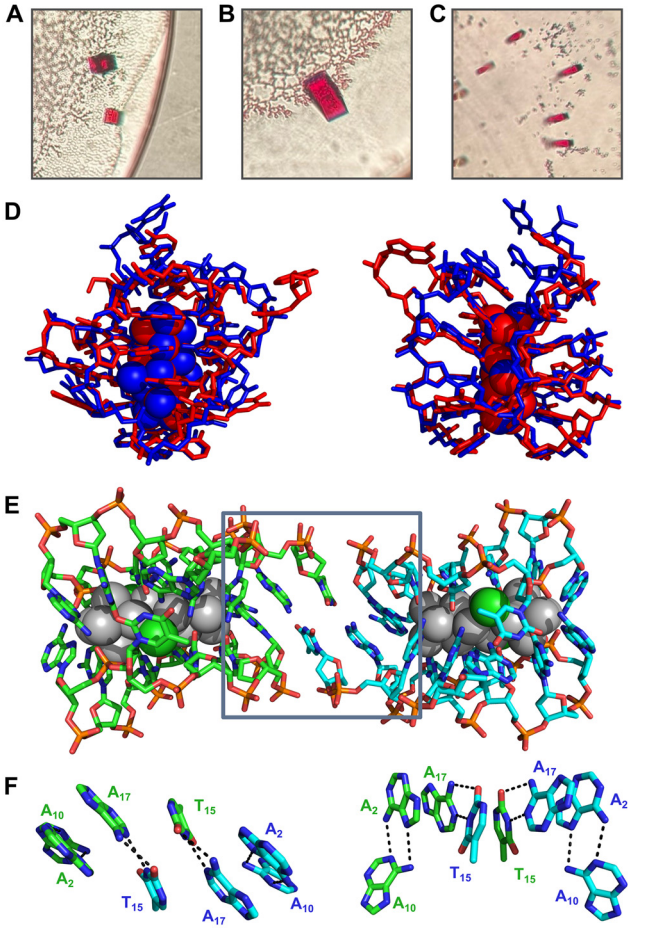

Fig. 3 Images of crystals of (A) 2xDNA(T_4)-$[Ag_{16}Cl_2]^{8+}$, (B) 2xDNA(T_5)-$[Ag_{16}Cl_2]^{8+}$and (C) 2xDNA(T_6)-$[Ag_{16}Cl_2]^{8+}$. (D) Crystal structure overlays of 2xDNA(T_5)-$[Ag_{16}Cl_2]^{8+}$ (blue, PBD: 9XV9) and DNA_2-$[Ag_{16}Cl_2]^{8+}$ units (red, PBD: 6JR4). (E and F) Detailed views of the crystal packing interactions in the 2xDNA(T_5)-$[Ag_{16}Cl_2]^{8+}$ structure.

times (Fig. S12). We managed to solve the structures of two of the three variants (2xDNA(T_5)-$[Ag_{16}Cl_2]^{8+}$ and 2xDNA(T_6)-$[Ag_{16}Cl_2]^{8+}$), which are deposited at the PDB website under accession codes 9XV9 and 9XVA, respectively.

For 2xDNA(T_5)-$[Ag_{16}Cl_2]^{8+}$, only T_{15} (the fifth T of the thymine segment) is visible in the structure due to a Watson–Crick interaction with an A_{17} of a neighbouring 2xDNA(T_5)-$[Ag_{16}Cl_2]^{8+}$ structure in the unit cell. For the rest, the positions of the Ag atoms and most of the DNA sequence overlap very well with the original DNA_2-$[Ag_{16}Cl_2]^{8+}$ nanocluster (see Fig. 3D). Fig. 3E and F show the intricate interactions between two 2xDNA(T_5)-$[Ag_{16}Cl_2]^{8+}$ units in the crystal. Unfortunately, the T_{11} to T_{14} nucleobases are too disordered to be resolved. This is reasonable given that no complementary nucleobases are available to form stable interactions with the thymine section, apart from the T_{15}–A_{17} interaction. For 2xDNA(T_6)-$[Ag_{16}Cl_2]^{8+}$, similar interactions were found (Fig. S13). Here, T_{15} and T_{16} could be resolved in the structure, but like in 2xDNA(T_5)-$[Ag_{16}Cl_2]^{8+}$, the T_{11} to T_{14} nucleobases could not be resolved. Results from Swasey *et al.* show that thymine strands

do not have a great affinity to form silver mediated duplexes,[26] while silver cations can easily replace a hydrogen to form adenine and thymine silver-mediated Watson–Crick-like interactions.[26,27] Silver-mediated thymine–thymine interactions have been previously reported by Kondo *et al.* but require the deprotonation of one of the thymines.[28,29]

Conclusions

In this work, we successfully designed and characterized single-stranded DNA-oligomer versions of the well-established DNA_2-$[Ag_{16}Cl_2]^{8+}$ nanocluster. By connecting the two native stabilizing strands through thymine linkers of defined lengths (T_4, T_5 and T_6), we created a single oligonucleotide that retains the structural and photophysical integrity of the original system with the additional benefit of removing redundant labeling sites. This architecture opens the door for precise, site-specific future conjugation strategies. Single crystal X-ray diffraction of the 2xDNA(T_5)-$[Ag_{16}Cl_2]^{8+}$ and 2xDNA(T_6)-$[Ag_{16}Cl_2]^{8+}$ variants yielded two crystal structures that closely resemble the original DNA_2-$[Ag_{16}Cl_2]^{8+}$ nanocluster, demonstrating that the overall $[Ag_{16}Cl_2]^{8+}$ core remains preserved. Although the engineered thymine segment was not fully resolved, the combination of mass spectrometry, single crystal x-ray diffraction based structure determination and spectroscopic measurements indicate that it does not interfere with the metal–DNA coordination environment or alter the core geometry.

Together, these results validate our design concept and highlight the feasibility of stabilizing the Ag_{16} cluster with a single DNA strand, thereby providing a robust and structurally conserved scaffold for controlled, one-site functionalization in future bioimaging applications. Furthermore, the presented approach could also be used as a testbed for other DNA sequences of limited length to investigate whether or not they interfere with AgNC formation.

Conflicts of interest

There are no conflicts to declare.

Data availability

The data supporting this article have been included as part of the supplementary information (SI). Supplementary information is available. See DOI: **https://doi.org/10.1039/d5qi02482j**.

Crystallographic data for 2xDNA(T_5)-$[Ag_{16}Cl_2]^{8+}$ and 2xDNA(T_6)-$[Ag_{16}Cl_2]^{8+}$ have been deposited at the PDB under accession codes 9XV9 and 9XVA.[30,31]

Acknowledgements

V. R. and T. V. acknowledge funding from the Villum Foundation (VKR023115), the Independent Research Fund Denmark (0136-00024B) and the Novo Nordisk Foundation (NNF22OC0073734). We acknowledge MAX IV Laboratory for time on Beamline Biomax under Proposal 20240265 allocated to Leila Lo Leggio. Research conducted at MAX IV, a Swedish national user facility, is supported by the Swedish Research Council under contract 2018-07152, the Swedish Governmental Agency for Innovation Systems under contract 2018-04969, and Formas under contract 2019-02496. MicroMAX is funded by the Novo Nordisk Foundation under grant number NNF17CC0030666. We are thankful for the assistance of Beamline Lead Jie Nan in operating the MicroMAX beamline. We thank the Danish Agency for Science, Technology, and Innovation for funding the instrument center DanScatt, supporting travel and sample shipping to synchrotrons and MAX IV staff for assistance during the beamtime. Z. H. was funded by the Independent Research Fund Denmark (Natural Sciences) under grant 3103-00279B. We thank Cecilia Cerretani for testing out some initial design ideas. J. K. and H. K. thank the Research Support Project for Life Science and Drug Discovery (Basis for Supporting Innovative Drug Discovery and Life Science Research (BINDS)) from AMED under Grant Number JP23ama121014.

References

1 J. T. Petty, J. Zheng, N. V. Hud and R. M. Dickson, DNA-Templated Ag Nanocluster Formation, *J. Am. Chem. Soc.*, 2004, **126**, 5207–5212.
2 A. Gonzàlez-Rosell, C. Cerretani, P. Mastracco, T. Vosch and S. M. Copp, Structure and luminescence of DNA-templated silver clusters, *Nanoscale Adv.*, 2021, **3**, 1230–1260.
3 Y. Zhang, C. He, K. de La Harpe, P. M. Goodwin, J. T. Petty and B. Kohler, A single nucleobase tunes nonradiative decay in a DNA-bound silver cluster, *J. Chem. Phys.*, 2021, **155**, 094305.
4 J. Sharma, H.-C. Yeh, H. Yoo, J. H. Werner and J. S. Martinez, A complementary palette of fluorescent silver nanoclusters, *Chem. Commun.*, 2010, **46**, 3280–3282.
5 R. R. Ramazanov, R. T. Nasibullin, D. Sundholm, T. Kurtén and R. R. Valiev, Nonradiative Deactivation of the Fluorescent Ag16-DNA and Ag10-DNA Emitters: The Role of Water, *J. Phys. Chem. Lett.*, 2024, **15**, 10710–10717.
6 A. Gonzàlez-Rosell and S. M. Copp, An Atom-Precise Understanding of DNA-Stabilized Silver Nanoclusters, *Acc. Chem. Res.*, 2024, **57**, 2117–2129.
7 S. Choi, R. M. Dickson and J. Yu, Developing luminescent silver nanodots for biological applications, *Chem. Soc. Rev.*, 2012, **41**, 1867–1891.
8 V. Rück, N. K. Mishra, K. K. Sørensen, M. B. Liisberg, A. B. Sloth, C. Cerretani, C. B. Mollerup, A. Kjaer, C. Lou, K. J. Jensen and T. Vosch, Bioconjugation of a Near-Infrared DNA-Stabilized Silver Nanocluster to Peptides and Human Insulin by Copper-Free Click Chemistry, *J. Am. Chem. Soc.*, 2023, **145**, 16771–16777.

9 G. Romolini, H. Kanazawa, C. B. Mollerup, M. B. Liisberg, S. W. Lind, Z. Huang, C. Cerretani, J. Kondo and T. Vosch, Shining Bright at 960 nm: A 28-Silver-Atom Nanorod Stabilized by DNA, *Small Struct.*, 2025, **6**, 2500022.

10 J. Yu, S. Choi, C. I. Richards, Y. Antoku and R. M. Dickson, Live Cell Surface Labeling with Fluorescent Ag Nanocluster Conjugates, *Photochem. Photobiol.*, 2008, **84**, 1435–1439.

11 J. Yu, S. Choi and R. M. Dickson, Shuttle-Based Fluorogenic Silver-Cluster Biolabels, *Angew. Chem., Int. Ed.*, 2009, **48**, 318–320.

12 S. M. Copp, D. Schultz, S. Swasey, J. Pavlovich, M. Debord, A. Chiu, K. Olsson and E. Gwinn, Magic Numbers in DNA-Stabilized Fluorescent Silver Clusters Lead to Magic Colors, *J. Phys. Chem. Lett.*, 2014, **5**, 959–963.

13 S. M. Copp, A. Gorovits, S. M. Swasey, S. Gudibandi, P. Bogdanov and E. G. Gwinn, Fluorescence Color by Data-Driven Design of Genomic Silver Clusters, *ACS Nano*, 2018, **12**, 8240–8247.

14 S. M. Copp, P. Bogdanov, M. Debord, A. Singh and E. Gwinn, Base Motif Recognition and Design of DNA Templates for Fluorescent Silver Clusters by Machine Learning, *Adv. Mater.*, 2014, **26**, 5839–5845.

15 R. Guha, A. Gonzàlez-Rosell, M. Rafik, N. Arevalos, B. B. Katz and S. M. Copp, Electron count and ligand composition influence the optical and chiroptical signatures of far-red and NIR-emissive DNA-stabilized silver nanoclusters, *Chem. Sci.*, 2023, **14**, 11340–11350.

16 J. T. Petty, B. Giri, I. C. Miller, D. A. Nicholson, O. O. Sergev, T. M. Banks and S. P. Story, Silver Clusters as Both Chromophoric Reporters and DNA Ligands, *Anal. Chem.*, 2013, **85**, 2183–2190.

17 C. Cerretani and T. Vosch, Switchable Dual-Emissive DNA-Stabilized Silver Nanoclusters, *ACS Omega*, 2019, **4**, 7895–7902.

18 P. Mastracco and S. M. Copp, Beyond nature's base pairs: machine learning-enabled design of DNA-stabilized silver nanoclusters, *Chem. Commun.*, 2023, **59**, 10360–10375.

19 C. Cerretani, H. Kanazawa, T. Vosch and J. Kondo, Crystal structure of a NIR-Emitting DNA-Stabilized Ag16 Nanocluster, *Angew. Chem., Int. Ed.*, 2019, **58**, 17153–17157.

20 S. A. Bogh, M. R. Carro-Temboury, C. Cerretani, S. M. Swasey, S. M. Copp, E. G. Gwinn and T. Vosch, Unusually large Stokes shift for a near-infrared emitting DNA-stabilized silver nanocluster, *Methods Appl. Fluoresc.*, 2018, **6**, 024004.

21 A. Gonzàlez-Rosell, S. Malola, R. Guha, N. R. Arevalos, M. F. Matus, M. E. Goulet, E. Haapaniemi, B. B. Katz, T. Vosch, J. Kondo, H. Häkkinen and S. M. Copp, Chloride Ligands on DNA-Stabilized Silver Nanoclusters, *J. Am. Chem. Soc.*, 2023, **145**, 10721–10729.

22 C. He, P. M. Goodwin, A. I. Yunus, R. M. Dickson and J. T. Petty, A Split DNA Scaffold for a Green Fluorescent Silver Cluster, *J. Phys. Chem. C*, 2019, **123**, 17588–17597.

23 D. J. E. Huard, A. Demissie, D. Kim, D. Lewis, R. M. Dickson, J. T. Petty and R. L. Lieberman, Atomic Structure of a Fluorescent Ag8 Cluster Templated by a Multistranded DNA Scaffold, *J. Am. Chem. Soc.*, 2019, **141**, 11465–11470.

24 F. Guay and A. L. Beauchamp, Model compounds for the interaction of silver(I) with polyuridine. Crystal structure of a 1 : 1 silver complex with 1-methylthymine, *J. Am. Chem. Soc.*, 1979, **101**, 6260–6263.

25 R. Guha, M. Rafik, A. Gonzàlez-Rosell and S. M. Copp, Heat, pH, and salt: synthesis strategies to favor formation of near-infrared emissive DNA-stabilized silver nanoclusters, *Chem. Commun.*, 2023, **59**, 10488–10491.

26 S. M. Swasey, L. E. Leal, O. Lopez-Acevedo, J. Pavlovich and E. G. Gwinn, Silver(I) as DNA glue: Ag+-mediated guanine pairing revealed by removing Watson-Crick constraints, *Sci. Rep.*, 2015, **5**, 10163.

27 C. López-Chamorro, A. Pérez-Romero, A. Domínguez-Martín, U. Javornik, O. Palacios, J. Plavec and M. A. Galindo, Silver Binding Dichotomy for 7-Deazaadenine/Thymine: Preference for Watson–Crick Pairing over Homobase Interactions in DNA, *Inorg. Chem.*, 2025, **64**, 14455–14465.

28 J. Kondo, Y. Tada, T. Dairaku, Y. Hattori, H. Saneyoshi, A. Ono and Y. Tanaka, A metallo-DNA nanowire with uninterrupted one-dimensional silver array, *Nat. Chem.*, 2017, **9**, 956–960.

29 B. Sengupta, C. M. Ritchie, J. G. Buckman, K. R. Johnsen, P. M. Goodwin and J. T. Petty, Base-Directed Formation of Fluorescent Silver Clusters, *J. Phys. Chem. C*, 2008, **112**, 18776–18782.

30 9XV9: Rück *et al.*, Bridging the gap: thymine segments to create single-stranded versions of DNA_2-$[Ag_{16}Cl_2]^{8+}$, 2026, DOI: **10.2210/pdb9XV9/pdb**.

31 9XVA: Rück *et al.*, Bridging the gap: thymine segments to create single-stranded versions of DNA_2-$[Ag_{16}Cl_2]^{8+}$, 2026, DOI: **10.2210/pdb9XVA/pdb**.